Available online at www.sciencedirect.com
SCIENCE DIRECT®
Archives of Biochemistry and Biophysics 428 (2004) 144–153
ABB
www.elsevier.com/locate/yabbi

A novel UV laser-induced visible blue radiation from protein crystals and aggregates: scattering artifacts or fluorescence transitions of peptide electrons delocalized through hydrogen bonding?

Anshuman Shukla, Sourav Mukherjee, Swati Sharma, Vishal Agrawal, K.V. Radha Kishan, and P. Guptasarma*

Institute of Microbial Technology, Sector 39-A, Chandigarh 160 036, India

Received 1 March 2004, and in revised form 30 April 2004
Available online 19 June 2004

Abstract

Proteins lacking prosthetic groups and/or cofactors are known to undergo electronic excitation transitions only upon exposure to UV-C (<280 nm) and UV-B (280–320 nm), but not UV-A (320–400 nm) photons. Here, we report the discovery of a novel excitation that peaks at ~340 nm and yields visible violet-blue radiation with apparent band maxima at ~425, 445, 470, and 500 nm. All proteins and large polypeptides examined in solid form, and in solutions, display this quenchable and photobleachable radiation which can be established not owing to aromatic sidechains. As a note of caution, we wish to state that we have not been able to completely eliminate the possibility that the radiation may be an artifact owing to second order effects such as, e.g., Raman scattering of Raman-scattered photons; however, we assert that all our experiments indicate that the radiation actually owes to some form of fluorescence. We propose that peptide electrons that have been delocalized through intramolecular or intermolecular hydrogen bond formation display these long-wavelength electronic transitions. If confirmed by future studies, this preliminary discovery may turn out to have important implications for biomolecular spectroscopy, protein crystallography, and materials science.

Keywords: Peptide fluorescence; Delocalized electrons; Blue radiation; UV illumination

Initial observations of a novel violet-blue fluorescence from protein aggregates were made entirely serendipitously on a fluorescence microscope during visual examination of the binding of a conditionally fluorescent dye (Congo red [1]) to the aggregated form of a globular protein, gamma-II crystallin, in our laboratory. We noted that before the addition of the dye control samples of aggregated gamma-II crystallin emitted a visible violet-blue radiation upon illumination with UV (350–390 nm), whereas the rest of the visual field remained dark; upon addition of the dye, this violet-blue fluorescence was gradually replaced by the characteristic pink-red fluorescence of the dye. Considering that proteins lacking cofactors and/or prosthetic groups have never been reported previously to emit visible violet-blue fluorescence, or indeed any form of visible fluorescence [2], and considering further that proteins are not known to support any electronic excitation whatsoever in this range of UV wavelengths, we reckoned initially that we could be observing one of the following three trivial phenomena; (i) an unusual Raman scatter of the long-wavelength (390 nm) component of the broad-band (350–390 nm) emission falling upon the solid protein sample, (ii) fluorescence emission emanating from unknown chemical groups attached to gamma-II crystallin's sidechains, derived through ageing-related chemical modifications of proteins in eye lens tissues, or (iii) fluorescence emission from photoproducts created through UV-mediated photolysis of

* Corresponding author. Fax: +91-172-2690-585.
E-mail address: pg@imtech.res.in (P. Guptasarma).

0003-9861/$ - see front matter © 2004 Elsevier Inc. All rights reserved.
doi:10.1016/j.abb.2004.05.007

aromatic amino acids. The last of these three possibilities, however, appeared remote because the blue radiation could be seen simultaneously with the switching on of the UV illumination, and did not increase in intensity during observation (as it should have, if it were being progressively created through UV irradiation). Also, the question of the radiation owing to diffraction effects originating in optical devices such as diffraction gratings and the like did not arise since the blue fluorescence was also visible to the naked eye beholding the sample on the slide placed on the microscope stage. In separate experiments that were essentially similar in design, we also later saw the same violet-blue radiation emanating from an aggregated sample of a 'designer' protein [the purified, recombinant, backbone-reversed form of the *Escherichia coli* protein, cold-shock protein A (retro-CspA)]. The observation of the very same radiation from two samples prepared by very different means caused us to further explore the phenomenon, using a Carl Zeiss LSM-510 Meta laser scanning confocal microscope equipped with spectrofluorimetric capability.

Here, we propose that the violet-blue radiation is actually fluorescence, and provide evidence to argue that UV-A illumination causes electronic excitations to occur in peptide bonds participating in hydrogen bond formation associated with protein secondary structures, with hydrogen bonds causing the necessary delocalization of peptide electrons to effect such long-wavelength low-energy transitions.

Materials and methods

Proteins and peptides

Gamma-II crystallin was purified from ovine lens tissue as described in previous work [3]. A peptide fragment of gamma-II crystallin, namely N-NDSIRSCRLIPQHT-C, lacking tryptophan, tyrosine as well as phenylalanine residues, was custom-synthesized by Mimotopes (Australia); this peptide has also been described in a previous work [3]. Whole length triosephosphate isomerase from *Pyrococcus furiosus* (*Pfu* TIM), and a 45-residue-long N-terminal fragment of this $(\beta/\alpha)_8$-barrel protein consisting of its first β/α unit and second β strand (i.e., $\beta_1\alpha_1\beta_2$) were separately obtained through PCR amplification of the relevant encoding DNA from *P. furiosus* genomic DNA (gift from Michael Adams, Athens, Georgia) and cloning and production in *E. coli* in fusion with a 12-residue-long N-terminal affinity tag (MRGSHHHHHHGS) through insertion into the pQE-30 expression vector (Qiagen). Backbone-reversed *E. coli* cold-shock protein A (retro-CspA) was similarly obtained through expression of a synthetic gene inserted into pQE-30 [4]. Details of recombinant hydantoinase have already been described in previous work [5]. The protein, lysozyme, and the peptide, glutathione, were commercially obtained from Sigma Chemical (St. Louis, MO, USA).

Aggregates, crystals, and lyophilized powders

Aggregates were examined by placing the same under coverslips, and examining slides on upright or inverted microscopes, using routine or confocal spectral imaging modes, and using illumination from a halogen lamp, a mercury-arc lamp, or a laser as appropriate. In contrast, crystals were examined non-invasively through the direct placing of 24-well crystallization trays containing hanging-drop setups on the stage of the upright Zeiss Axioplan2 microscope. Aggregates of gamma-II crystallin were created by heating 0.7 mg/ml solutions at 70 °C for 30 min, and sedimenting and harvesting thermally aggregated protein through centrifugation. Aggregates of retro-CspA were obtained by harvesting of sediments resulting from centrifugal vacuum-based concentration of solutions to concentrations exceeding 1.5 mg/ml, at physiological pH, since this protein precipitates above this concentration (unpublished observations). Crystals of lysozyme were obtained by standard methods. Hydantoinase crystals were obtained as described previously [4]. Crystals of the two recombinant *P. furiosus* proteins were obtained under conditions that will be described elsewhere. Salt crystals were obtained from various hanging-drop crystallization setups.

Microscopes

Initial observations were made using a Nikon Eclipse E-600 fluorescence microscope with an FDX-35 film camera. All subsequent routine fluorescence microscopy, as also confocal microscopy, was carried out either using the upright Carl Zeiss Axioplan2 microscope, or the inverted Carl Zeiss Axiovision microscope. Confocal laser imaging was done using the LSM-510 Meta laser scanning head. Ordinary photographic images under halogen/mercury lamp illumination were collected using the Carl Zeiss AxioCam digital camera on the Axioplan2.

Lasers, lamps, and optical filters

The UV laser used with the LSM-510 Meta (Coherent Enterprise II 653) emits two lines, at 351 and 364 nm, and no other lines in the UV or visible regions of the EM spectrum (details of the laser can be viewed at http://www.laser-innovations.co.uk/support/download/enterprise_DS. pdf). This laser was used for UV illumination during confocal spectral imaging, to create all the data

shown in Fig. 1 (all panels), Fig. 3 (panels B, C, E, and F), Fig. 4 (all panels), Fig. 5 (all panels), and Fig. 6 (all panels). A filter allowing light of >385 nm was used to prevent the Rayleigh-scattered laser light from reaching the detector; separately, radiation of any wavelength range could be monitored using the Meta attachment of the instrument that functions like a prism-based emission monochromator. To collect visible light-scatter images of crystals shown in Fig. 3 (panels A and D), a 488 nm laser line from a different laser was separately used. For photographic imaging and viewing with visible light, either singly (panels G and J) or in combination with UV illumination (panels H and K), the regular halogen lamp of the microscope was used for generating data shown in Fig. 3; similarly for fluorescence imaging under UV illumination, either singly (panels I and L) or in combination with visible illumination from the halogen lamp (panels H and K), the mercury lamp of the microscope was used for generating data shown in Fig. 3. The mercury-arc lamp was used with a 364 nm filter and a 13 nm bandpass, additionally restricting light falling on the sample to the wavelength range of 359–371 nm.

Elimination of Raman scattering as a possible explanation

Separate illumination effected with two different laser lines differing by 13 nm is expected to give rise to

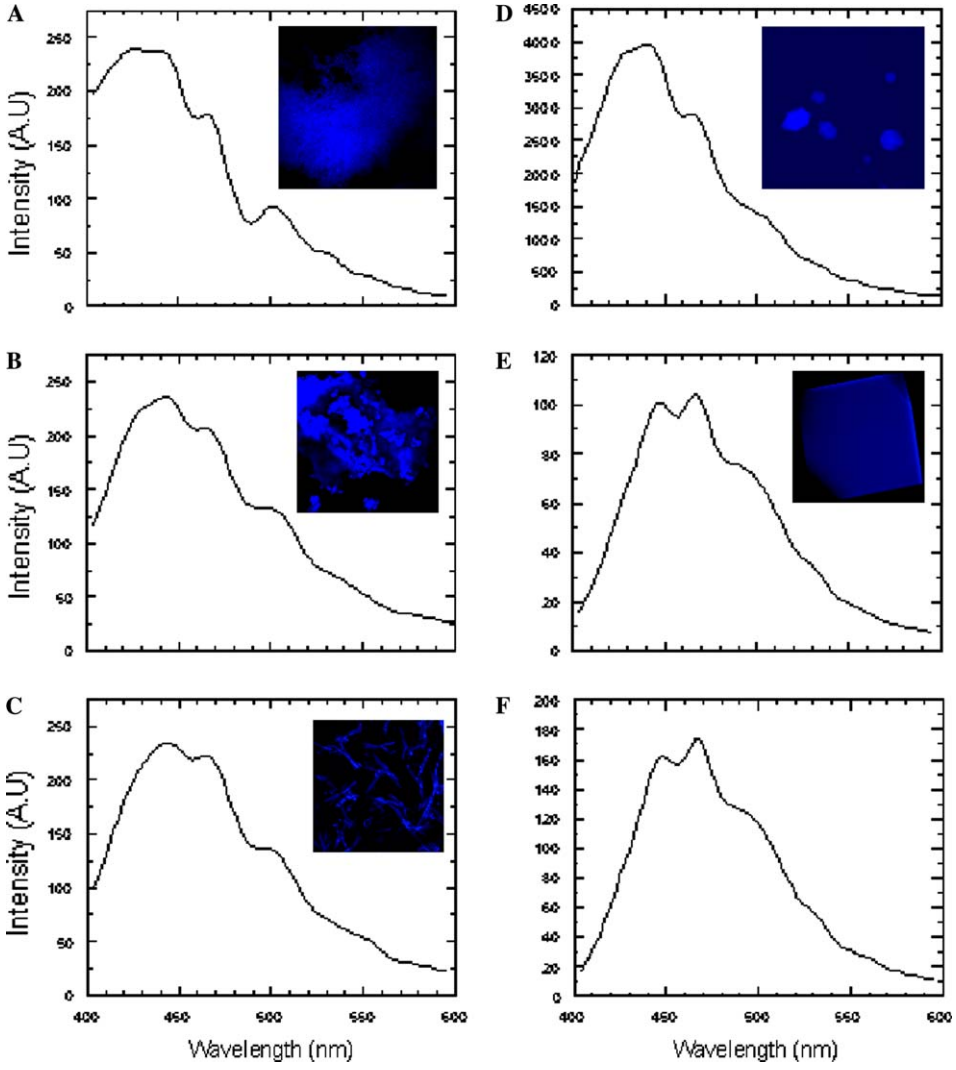

Fig. 1. Blue fluorescence emission from proteins. Panels show fluorescence emission spectra of different proteins upon excitation with the combined 351/364 nm lines of a UV laser using a Carl Zeiss LSM-510 Meta confocal spectral imaging microscope (see Materials and methods). Insets show false-colour intensity-coded blue images of emission collected using a longpass filter (>385 nm). (A) Lyophilized (powder) form of a synthetic peptide lacking aromatic residues derived from an all-beta protein, gamma-II crystallin. (B) Thermally precipitated gamma-II crystallin from ovine lenses. (C) Needle-like crystals of recombinant *P. furiosus* TIM, affinity purified from overexpressing *E. coli*. (D) Crystals of recombinant *Bacillus* sp. AR9 hydantoinase purified from *E. coli*. (E) Crystals of commercially obtained chicken egg white lysozyme (excited with only the 351 nm laser line). (F) Same sample as in (E) (excited with only the 364 nm laser line). Although all samples show the same bands, relative intensities of bands vary amongst samples.

proportionately different wavelengths of maximal radiation (λ_{max}), if Raman scattering is responsible, whereas no change in λ_{max} can be anticipated if fluorescence is responsible. We used the two laser lines to examine whether there is any change in λ_{max}. Representative data with lysozyme crystals are shown in Figs. 1E and F.

Elimination of aromatics and/or their photoproducts as possible origins of radiation

We inspected a sample lacking all the three aromatic amino acids which absorb and fluoresce in the UV-B range, i.e., tryptophan (Trp), tyrosine (Tyr), and phenylalanine (Phe), to investigate whether photoproducts of the aromatic residues might be responsible for the observed radiation. It is worth noting that the aromatic residues themselves, in any case, do not absorb UV-A radiation, or fluoresce in the visible region, causing us to be concerned mainly about possible photoproducts; however, by using samples lacking aromatics, the remote possibility that the radiation owes to a low-probability aromatic transition too could be examined. Representative data with one such sample, a synthetic polypeptide derived from gamma-II crystallin, which lacks aromatics, are shown in Fig. 1A.

Elimination of the peptide bond moiety as a possible origin of radiation

Apart from aromatic residues, the only other moiety that absorbs radiation in the UV above 200 nm in proteins and polypeptides is the peptide bond, which

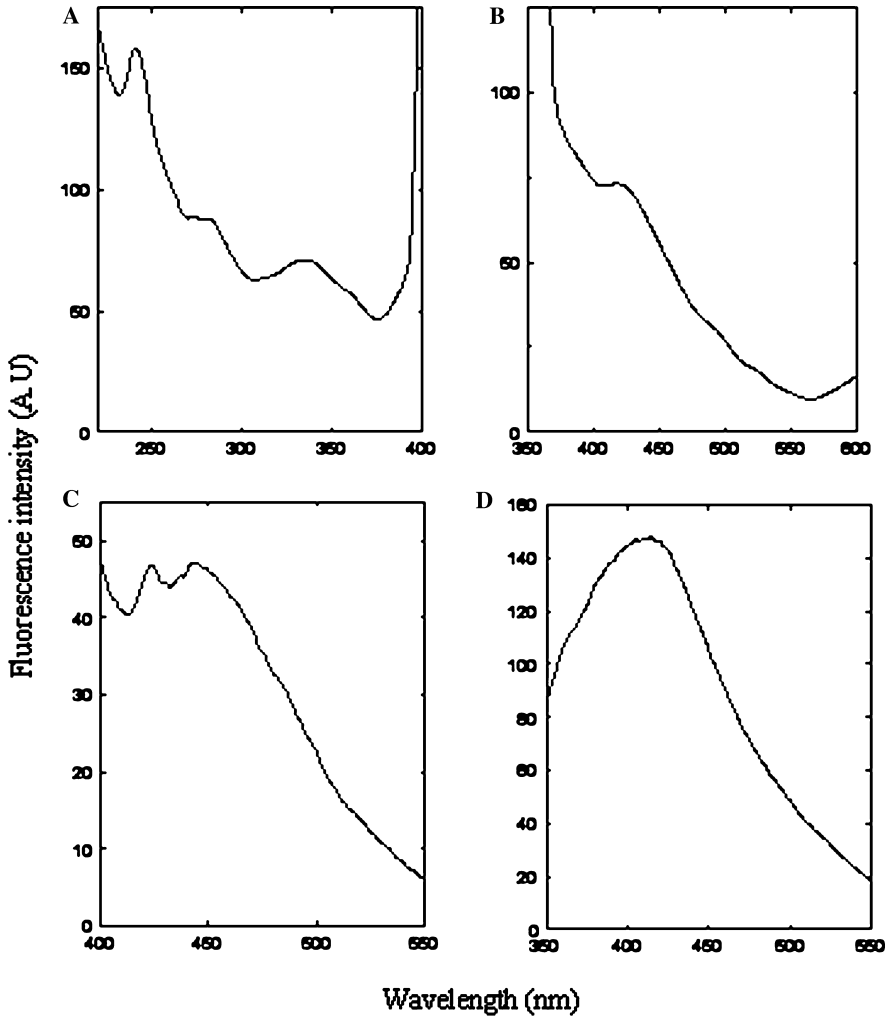

Fig. 2. Excitation and emission spectra of protein/peptide samples in water, displaying characteristics of non-aromatic visible violet-blue emission, using different monochromator (MC) and bandpass (BP) settings, as specified below. (A) Excitation spectrum (15 nm BP) of truncated ($\beta_1\alpha_1\beta_2$) *P. furiosus* TIM, with emission MC set at 420 nm (15 nm BP). (B) Emission spectrum (15 nm BP) of truncated ($\beta_1\alpha_1\beta_2$) *P. furiosus* TIM, with excitation MC set at 340 nm (15 nm BP). (C) Emission spectrum (3 nm BP) of gamma-II crystallin, with excitation MC set at 240 nm (3 nm BP). (D) Emission spectrum (8 nm BP) of the 14-mer, aromatic residue lacking peptide shown in (A), Fig. 1, with excitation MC set at 240 nm (3 nm BP). The excitation spectrum was characteristic of all samples.

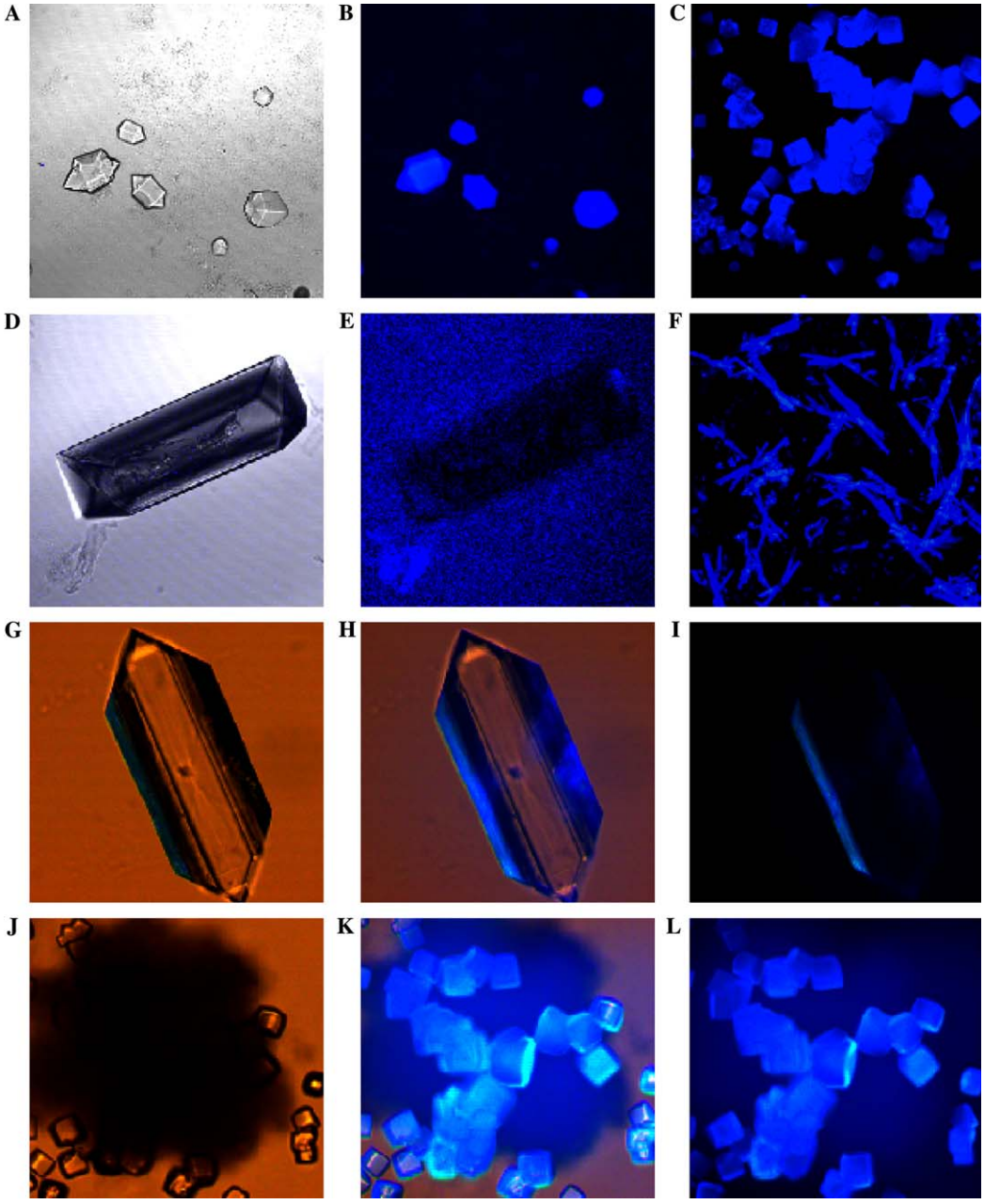

Fig. 3. Comparison of images of salt and protein crystals collected non-invasively by mounting trays of 'hanging-drop' crystallization plates on the upright (Axioplan2) Carl Zeiss LSM-510 Meta. For these images, illumination was effected with either laser light from visible (488 nm) or UV (364) sources, or with broad-band visible (halogen) or UV (mercury arc; UV filter) lamps. (A) Hydantoinase imaged using scatter of 488 nm laser light at low intensity. (B) Hydantoinase excited with 364 nm and in fluorescent mode (imaged with >385 nm longpass filter). (C) Truncated ($\beta\alpha\beta$) *P. furiosus* TIM excited with 364 nm (imaged as in B). (D) $MgCl_s$ imaged using scatter of 488 nm laser light (as in A). (E) $MgCl_2$ excited with 364 nm (imaged with a >385 nm filter, as in C). (F) Whole-length *P. furiosus* TIM excited with 364 nm (imaged as in B). (G) $LiCl_2$ under halogen lamp. (H) $LiCl_2$ under halogen and mercury-arc lamp. (I) $LiCl_2$ under mercury-arc lamp. (J) Truncated ($\beta_1\alpha_1\beta_2$) *P. furiosus* TIM under halogen lamp. (K) Truncated ($\beta_1\alpha_1\beta_2$) *P. furiosus* TIM under halogen and mercury-arc lamps. (L) Truncated ($\beta_1\alpha_1\beta_2$) *P. furiosus* TIM under mercury-arc lamp. Only protein crystals and protein adsorbed onto salt crystals are observed to fluoresce. The salt crystals themselves show no fluorescence.

absorbs UV-C radiation. However, to examine whether the peptide bond per se displays a low-probability UV-A absorption transition, we inspected the lyophilized powder form of a small synthetic peptide, glutathione [6], containing three amino acids, i.e., γ-glutamic acid, glycine, and cysteine.

Examination of quenching of radiation

Fluorescence quenching [7] using potassium iodide (KI) was used to visually examine whether quenching of radiation could be observed, since only fluorescence and not scattering would show quenching. Represen-

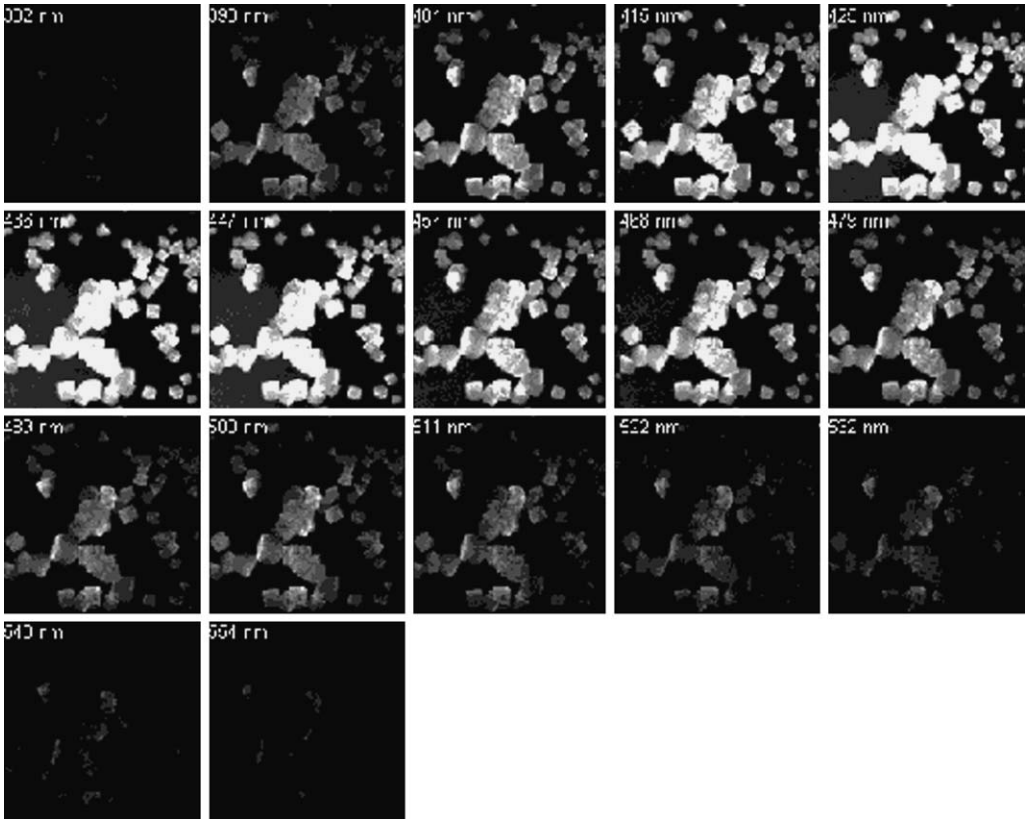

Fig. 4. A gallery of spectrally defined images (magnification 10×) collected using the LSM-510 Meta from a visual field of truncated ($\beta_1\alpha_1\beta_2$) *P. furiosus* TIM crystals emitting upon excitation with a 364 nm laser line. Intensity is represented as brightness in black-and-white images. The panels (in the order: left-to-right, top-to-bottom) show accumulated 10.5 nm bandwidth emissions centred at 382, 393, 404, 415, 425, 436, 447, 457, 468, 479, 489, 500, 511, 522, 532, 543, and 554 nm, respectively.

tative quenching data with retro-CspA aggregates are shown in Fig. 5. Aggregated material suspended in water (7 μl) was deposited onto a slide and placed under a coverslip. A 2.5 μl volume of KI (2.5 M, containing 1 mM $Na_2S_2O_3$) was diffused in from the coverslip's edge. Images were collected as a time series, at 0, 3.53, 7.06, and 10.59 s as shown in the figure.

Examination of photobleaching of radiation

The techniques of photobleaching (PB) and fluorescence recovery after photobleaching (FRAP) using high-intensity laser radiation [8] were used to examine whether samples show photobleaching and recovery. Representative data with photobleaching and recovery of aggregated $\beta_1\alpha_1\beta_2$ *P. furiosus* TIM are shown in Fig. 6. The sample was illuminated (only in the region shown in the rectangular box) with a pinhole dimension of 1000 μm for a period of 40 min using the maximum possible intensity of the UV laser, and both its 351 and 364 nm lines. Subsequently, the sample was examined after 15 and 30 min of remaining without illumination.

Measurement of the radiation spectrum

The spectral imaging capability of the Zeiss LSM-510 Meta was used to characterize the wavelength range of the observed radiation as shown in all panels in Fig. 1. Details of this capability can be viewed on the web at URL http://www.zeiss.de/de/micro/home_e.nsf. For spectrofluorimetry of proteins in solution, as shown in Fig. 2, a Perkin–Elmer LS-50B fluorimeter was used.

Results and discussion

We found that all forms of solid protein samples examined display the violet-blue radiation (Fig. 1). In all samples, local band maxima (λ_{max}) were seen at ~425, 445, 470, and 500 nm, with relative intensities varying from one sample to another such that different samples showed different absolute maxima. A synthetic lyophilized 14-mer peptide lacking aromatic residues (panel A) showed an absolute λ_{max} at 425 nm. A thermally aggregated sample of gamma-II crystallin (panel B), as well as crystals (panel C) of recombinant *P. furiosus* triosephosphate isomerase (TIM), displayed an absolute

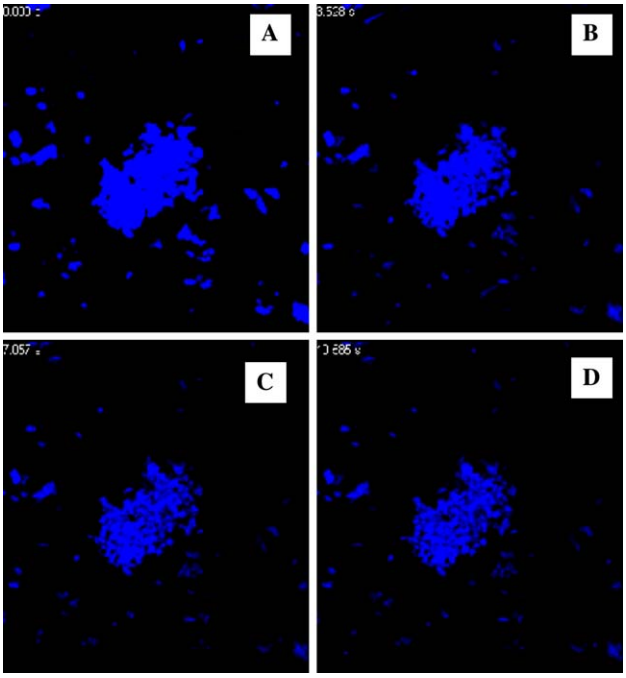

Fig. 5. Quenching of blue fluorescence emission (for details see Materials and methods). The instrument setup was similar to that used to collect the image in Fig. 3B. Quenching is shown as a time series of images. The sample is deliberately excited with high-laser power to effect high intensity with blurred detail in (A), to improve contrast in (B–D) through quenching. Greater detail is visible upon quenching.

λ_{max} at 445 nm. The crystalline form of commercially procured chicken egg white lysozyme (panels E and F) displayed the absolute λ_{max} at 470 nm. A small peptide regulator of intracellular redox potential, glutathione, did not show any detectable fluorescence at all; data are not shown because the entire field containing glutathione powder remained dark even at the highest allowed laser intensities of 351 and/or 364 nm illumination.

Proteins in aqueous solution examined using a spectrofluorimeter also showed this radiation, regardless of the details of the buffer system used. Some representative samples are shown in Fig. 2. To avoid possible spectral contamination by the Raman scatter of long-wavelength tryptophan emission, a recombinant, truncated ($\beta_1\alpha_1\beta_2$) form of *P. furiosus* TIM produced in our laboratory that contains only tyrosine and phenylalanine but no tryptophan residues was seen to emit the violet-blue radiation with the absolute λ_{max} at ~425 nm upon illumination with any wavelength of UV from over a broad range of wavelengths (panel A). It may be noted that in this 'excitation spectrum,' several wavelengths of illumination elicit peaks of the blue-violet radiation, including one local λ_{max} at ~340 nm. When this truncated form of TIM is illuminated specifically with 340 nm, violet-blue radiation with an absolute λ_{max} at ~425 nm (panel B) is clearly discerned to separate away from the long-wavelength tail of the Rayleigh scatter owing to excitation with broad-band (15 nm bandpass) 340 nm UV light. Since the excitation spectrum suggests that an even greater intensity of radiation at ~420 nm is stimulated by 240 nm illumination (possibly owing to excitation of peptide bonds, which absorb at these wavelengths) than by 340 nm illumination, two other samples were illuminated with 240 nm photons to maximize the intensity observed and improve the signal/noise ratio (panels C and D). One of these, gamma-II crystallin (panel C), is seen clearly to emit violet-blue radiation with one local λ_{max} at ~425 nm and another at ~445 nm. Using 240 nm excitation (which can simultaneously stimulate UV emission from aromatics), of course, the violet-blue radiation is best observed when there is absolutely no accompanying UV fluorescence from aromatics. Thus, in an emission spectrum ranging from 350 to 550 nm, the 14-mer peptide lacking aromatics (see Fig. 1A) was seen to emit with an absolute λ_{max} at ~415–420 nm, with other contributions also visible within the spectral envelope. The violet-blue visible radiation appears to be stimulated, therefore, by UV photons from the entire range of ultraviolet, with excitation occurring maximally at ~240 and ~340 nm; an additional excitation maximum is observed at 280–285 nm (panel A), suggesting that aromatic excitation which peaks at these wavelengths too can contribute to the radiation although the presence of aromatics is evidently not necessary.

Further proof that the radiation is seen only from proteins but not from other substances is presented in Fig. 3. A variety of images of protein crystals, protein aggregates, and salt crystals (from crystallization hanging-drop preparations) are shown. The samples either fluoresce brightly upon UV illumination, or do not fluoresce at all, depending on whether or not they contain any proteinaceous material. Some images which are in false-colour (panels B, C, E, and F) were collected using the LSM-510 confocal microscope; these represent only intensity-coded data of the >385 nm radiation resulting from excitation by the 364 nm (UV laser) in a single confocal plane. The corresponding visible light (Rayleigh scatter, 488 nm laser) images from the same confocal planes are shown for comparison, in the case of two samples (for panel B in panel A, and for panel E in panel D). Separately, true-colour photographs of crystals and aggregates (panels G–L) were collected using the digital (Axiovision) camera of the LSM-510 Meta instrument in the routine optical microscopic mode rather than the confocal scanning mode. As detailed in the Materials and methods section, photographs used one of the following: only visible illumination from the halogen lamp (panels G and J), only UV illumination from the mercury-arc lamp through a 359–371 nm filter (panels I and L), or a combination of both (panels H and K). In summary, all images demonstrate that salt crystals do not fluoresce at all under UV illumination (panels E, H, and I), whereas protein crystals (panels B, C, F, K, and

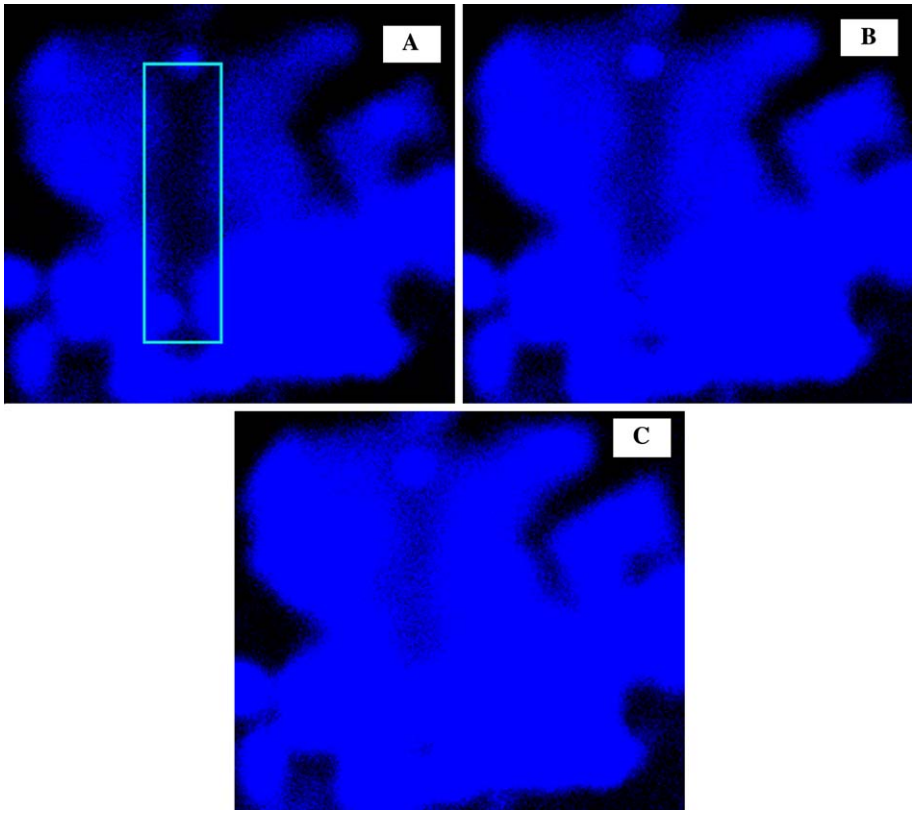

Fig. 6. Photobleaching and recovery. (A) An aggregate of $\beta_1\alpha_1\beta_2$ *P. furiosus* TIM was illuminated (only in the region shown in the rectangular box; with a pinhole of 1000 μm) for a period of 40 min using the maximum possible intensity of the UV laser, and both its 351 and 364 nm lines. The sample is shown with the photobleached region, depleted of fluorescence potential. Edges do not exactly correspond to the box because protein density was not identical in all parts of the sample. (B) The photobleached sample from the previous panel, 15 min after stopping of exposure to UV. (C) The sample after 30 min of stopping of exposure to UV. Fluorescence recovery after photobleaching (FRAP) is seen to progress in the boxed region. It is also seen to progress in neighbouring regions bleached partially by Rayleigh-scattered UV photons.

L) as well as aggregates of proteins in hanging-drop preparations that are either lying separately, or loosely associated with salt crystal surfaces (panels E, H, I, K, and L) display the violet-blue radiation regardless of the modes of excitation and detection used.

A series of selected wavelength-resolved images of protein crystals from one of the crystallization drops (collected using the Meta spectral imaging function of the LSM-510) is shown in Fig. 4, as visual evidence of variations in radiation intensity over the range of wavelengths from ~390 to 550 nm, as already indicated in the plotted data in Fig. 1.

That the violet-blue radiation is indeed fluorescence could be further established using two approaches. (i) *Quenching*. The probability of an electronic de-excitation transition occurring through fluorescence, rather than by other means, can be altered by the collision of the excited fluorescent moiety with a species such as the iodide ion. Fig. 5 shows a time series of photographs establishing the quenching of retro-CspA aggregates by KI. (ii) *Photobleaching and fluorescence recovery after bleaching.* Fluorophores exposed to high-intensity laser illumination of wavelength corresponding to that eliciting an absorption transition show a reduced ability to fluoresce for some time. Subsequently, there is a recovery of the ability to fluoresce. Fig. 6 shows photobleaching and FRAP results with precipitates of truncated TIM. The recovery could be arising from molecular dissociation–reassociation-based relocation of proteins in the sample. Alternatively, if the photobleaching mechanism in this instance does not owe to any covalent modification of the primary structure of the protein sample, recovery could be occurring through some form of replenishment of the region of the sample by electrons moving in from other regions of the sample through a hydrogen-bonding network (see later discussion). At any rate, regardless of the explanation for the recovery after photobleaching, the very observation of photobleaching would appear to rule out scattering as a cause of the radiation.

Since we appear to have established that the novel violet-blue radiation from proteins owes to fluorescence that does not originate in aromatic residues, but which displays excitation at wavelengths that also excite both peptide bonds and aromatic residues, it would appear as if the fluorescence were due to an intrinsic excitable

moiety present in all proteins, such as the peptide bond. That it cannot be due to a hitherto unnoticed low-probability electronic transition shown by the peptide bond per se, however, is established by the observation that a peptide-bond containing substance, glutathione, does not display the fluorescence. We propose the following explanation. Peptide bonds are known to have a partial double-bond character. The formation of hydrogen bonds by C═O and N─H atom groups from peptide bonds can potentially cause delocalization of some peptide orbital electrons. These delocalized electrons can potentially show low-probability excitation transitions at lower energies and wavelengths that are longer than those characteristic of normal absorption by peptides. They can also potentially de-excite partially through a fluorescence mechanism unlike ordinary peptide electrons which do not de-excite by fluorescent means. If this is the explanation of the fluorescence, it may be noted that the fluorescence would be shown by all samples containing peptides participating in hydrogen bonds; regardless of whether these were intramolecular or intermolecular, or in solid form or dissolved in aqueous solutions, or present in lyophilized powders with enough water content to facilitate intermolecular hydrogen bond formation, even amongst peptides with the propensity to form β sheets.

While the possibilities raised above are fundamentally interesting, we can think of at least three reasons why the discovery might also be important from the point of view of applications.

First, if it is true that H-bonded peptides support long-wavelength electronic excitations, proteins in solid form that are exposed to ultraviolet (whether from a specific source or to the UV component of daylight) could potentially support a network of delocalized electrons tunnelling through the peptide backbone and hydrogen bond networks, exchanging between different parts of a protein, or between molecules. This could make proteins, particularly amyloid fibres composed of cross β sheet structures, interesting materials from the viewpoint of electrical/electronic conduction.

Second, the discovery will make it a straightforward task for those attempting protein crystallization, who do not have immediate access to diffraction equipment, to determine non-invasively whether a crystal observed in a hanging drop is made of proteinaceous material or salt. Currently, relatively primitive and invasive methods are used for this purpose [9–11], involving: (a) physical crushing or dehydration of crystals, (b) gel electrophoresis of dissolved crystals, or (c) binding of dyes deposited into crystallization solutions.

Third, the variations in the intensities of the band maxima amongst samples (see Fig. 1), together with the proposed likelihood of the fluorescence owing to delocalized peptide orbital electrons, suggest that the fluorescence characteristics may be sensitive to secondary structure. Thus, the absolute λ_{max} of a protein could depend on the dominant form of secondary structure. From the data in Fig. 1, and those of other proteins (data not shown) we would venture to propose that β sheets give rise to lower wavelengths of fluorescence than α helices, such that the relative intensities at different wavelengths in the overall emission envelope might provide clues as to which secondary structure dominates a protein's structure. This possibility is being tested. We are also currently examining whether the apparently weaker fluorescence in solution is caused by the greater translational freedom of molecules that cause collisional de-excitations reducing the net probability of de-excitation occurring through fluorescence.

Finally, notwithstanding the important issue of whether the visible blue radiation is artifactual and scattering-based, or some novel form of fluorescence, the question still remains as to why it has remained undiscovered until now, since it can even be seen to emanate from solid protein samples illuminated with high-intensity UV light, by the naked eye. We think that the reason that it has remained undiscovered is that no reason has previously arisen to cause researchers to shine ultraviolet light of high intensity on solid protein samples, particularly from laser-based sources. It must also be mentioned that protein researchers tend to shine as little ultraviolet light on their samples as possible because broad-spectrum UV light can cause oxidative modifications of various sorts in proteins [12], especially if such light includes wavelengths capable of being absorbed by the peptide moiety, or by the aromatic amino acid residues in proteins. In the specific case of the laser used here, fortunately, the wavelengths available were 351 and 364 nm (note: these wavelengths are used for other applications, e.g., to excite DNA-binding dyes in studies of cell nuclei). These two wavelengths do not interact with any known moiety in proteins, making such a laser safe for use with protein samples.

Acknowledgments

This work was supported by grants to study protein folding and aggregation in P.G.'s laboratory from CSIR, New Delhi (New Idea Fund Grant, Young Scientist Award Grant), and INSA, New Delhi (Young Scientist Award Grant). A.S., S.M., and S.S. are doctoral research fellows supported by the CSIR in P.G.'s laboratory, and VA in K.V.R.K.'s laboratory.

References

[1] R.P. Linke, Highly sensitive diagnosis of amyloid and various amyloid syndromes using Congo Red fluorescence, Virchows Arch. 436 (2000) 439–448.

[2] G. Weber, F.W.J. Teale, Ultraviolet fluorescence of aromatic amino acids, Biochem. J. 65 (1957) 476–482.
[3] B. Kundu, A. Shukla, P. Guptasarma, Peptide scanning-based identification of regions of gamma-II crystallin involved in thermal aggregation: evidence of the involvement of structurally analogous helix-containing loops from the two double Greek key domains of the molecule, Arch. Biochem. Biophys. 410 (2003) 69–75.
[4] A. Shukla, M. Raje, P. Guptasarma, A backbone-reversed all-beta polypeptide (retro-CspA) folds and assembles into amyloid nanofibres, Protein Eng. 16 (2003) 875–879.
[5] V. Agrawal, R. Sharma, R.M. Vohra, K.V. Kishan, Crystallization and preliminary X-ray diffraction analysis of a thermostable D-hydantoinase from the mesophilic *Bacillus* sp. AR9, Acta Crystallogr. D Biol. Crystallogr. 58 (2002) 2175–2176.
[6] F.G. Hopkins, On glutathione: a reinvestigation, J. Biol. Chem. 84 (1929) 269–320.
[7] M.R. Eftink, C. Ghiron, Fluorescence quenching studies with proteins, Anal. Biochem. 114 (1981) 199–227.
[8] K. Jacobson, Z. Derzko, E.S. Wu, Y. Hou, G. Poste, Measurement of the lateral mobility of cell surface components in single, living cells by fluorescence recovery after photobleaching, J. Supramol. Struct. 5 (1976) 565–576.
[9] T.M. Bergfors, In Protein Crystallization: Techniques, Strategies and Tips, IUL Biotechnology Series (1999).
[10] Hampton Research. Crystallization: Research Tools 11 (2001) pp. 152–165.
[11] L. Cosenza, T. Bray, L.J. Delucas, T. Gester, D.T. Hamrick, International Patent No. PCT 02-13-03 03012430 WO NDN-172-0060-5579-4 (2003).
[12] D. Balasubramanian, P. Guptasarma, M. Luthra, In situ photoreactions of proteins in spectrometers leading to variations in signal intensities, J. Am. Chem. Soc. 114 (1992) 1878–1879.